A Comprehensive Guide to Angular Momentum

Opal Gordon
Editor

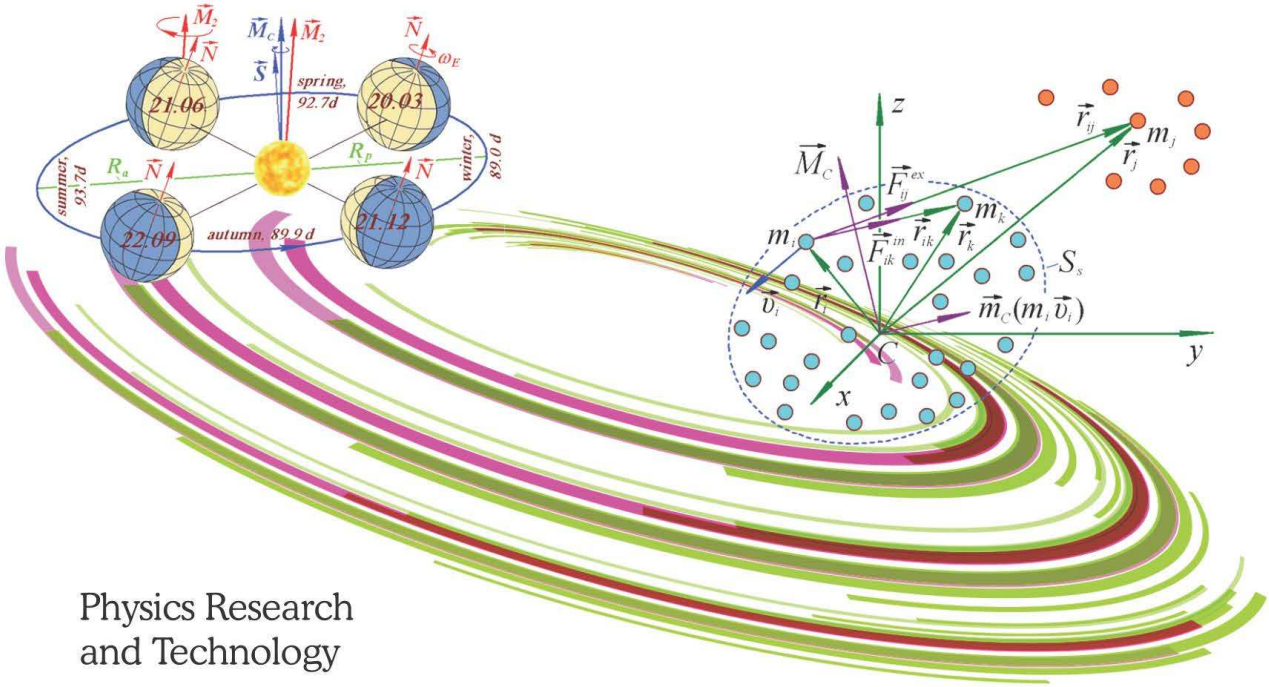

Physics Research and Technology

NOVA

In: A Comprehensive Guide to Angular… ISBN: 978-1-53615-707-9
Editor: Opal Gordon

Chapter 1

ANGULAR MOMENTUM DUE TO SOLAR SYSTEM INTERACTIONS.

Joseph J. Smulsky*
Institute of Earth's Cryosphere, Tyum SC of SB RAS,
Federal Research Center, Tyumen, Russia

ABSTRACT

Substantiations of the theorem of angular momentum change and the law of conservation of angular momentum are considered. The change of angular momentum indicates an error in the method of calculating the dynamics of the Solar system. In the Galactica program, the change in dimensionless angular momentum over 160 years is $2\ 10^{-21}$, whereas in programs using SDM, this change is within $8\ 10^{-10}$. The changes in angular momentum of individual bodies are analyzed, including the planets, the Sun and the Moon, as well as their influence on the changes in angular momentum of the Solar system. The variations in angular momentum due to the orbital motion of the planets relative to the Sun over various time intervals are considered. The evolution of angular momenta of the planets over millions of years proceeds through their clockwise procession around the total angular momentum of the Solar system. The angular momenta due to rotational motion of the planets and the Moon are analyzed.

* Corresponding Author address
Email: JSmulsky@mail.ru

Those momenta are five orders of magnitude smaller compared with the angular momenta due to the orbital motion. In the Galactica program, the angular momenta due to the rotational motion are taken into account at considering the processes of collision of bodies and their fusion into one body. The evolution of angular momentum due to the rotational motion of Earth over millions of years is analyzed. That angular momentum also precesses clockwise, as well as the angular momentum due to orbital motion, yet relative to another direction. The angle between the latter direction and the direction of total angular momentum of the Solar system is 3.2°. The reported results illustrate the specific features in the evolution of the Solar system. They can prove useful in controlling and improving the methods of calculation.

Keywords: differential equations, motions, angular momentum, orbits, rotation, axes, solution accuracy

INTRODUCTION

In mechanics, the interactions and motions of bodies are analyzed using two characteristics of their interaction: force and the moment of force. The translational movement of bodies is expressed as momentum, and the rotational motion, as angular momentum. The differential equations for translational motion stem from the fact that the presence of a force leads to a change in momentum. Similarly, the differential equations for rotational motion result from the fact that the presence of a moment of force leads to a change of angular momentum. In addition to the direct influence on rotational motion, angular momentum can also be used to control the translational motion and test the calculation methods for this motion.

The results of the space studies of recent decades provide evidence that the calculated orbits of celestial bodies and trajectories of spacecraft may often be inconsistent with their observed motions. Similar evidence is provided by studies of the Solar System's evolution over geological time periods. This evidence has led some researchers to conclude that the motions of objects in the Solar System are generally chaotic, suggesting a likelihood of a future collapse of the Solar System [1], chaotic motions of asteroids after planetary encounters [2], etc. Other researchers address these inconsistencies by introducing, in addition to the Newtonian force of gravity, other, weaker influences such as the Yarkovsky effect [3], dark matter [4], radiation pressure, etc.

However, the indeterminacy of motion and the unclear nature of the forces contradict the spirit of mechanics. Apparently, before accepting the above

changes, researchers need to check, within the framework of mechanics, the reliability of the existing methods for calculating motions. One measure as to whether the solution of a mechanics problem is accurate is the observance of the laws of conservation. In this paper, we investigate the conservation of angular momentum for the entire system of interacting bodies by different methods in calculating the dynamics of the Solar System.

THEOREM ON THE CHANGE OF ANGULAR MOMENTUM FOR A SYSTEM OF MATERIAL POINTS

Consider a mechanical system S_s involving N material points (Figure 1), where the numbers of the points are $i = k = 1, 2, \ldots N$. Each of the k points acts on point i with a force F_{ik}^{in}, where $k \neq i$. The superscript "*in*" denotes the force of interaction of the material points included in the system S_s. Those forces are *internal*, and they are characterized by the fact that the forces of mutual action are equal in magnitude and opposite in direction:

$$\vec{F}_{ik}^{in} = -\vec{F}_{ki}^{in}. \tag{1}$$

Expression (1) is known as the third law of mechanics.

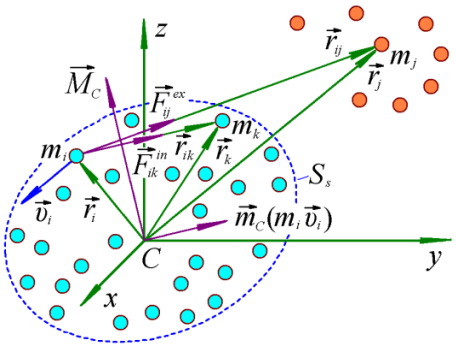

Figure 1. Interaction of bodies m_i of system S_s by internal forces F_{ik}^{in} and their interaction by external forces F_{ij}^{ex} with bodies m_j that are not included in the system of S_s.

In addition, outside system S_s there are J material points ($j = 1, 2, \ldots J$) (Figure 1), each acting on points m_i of system S_s with an external force F_{ij}^{ex}, where the subscript "*ex*" (*external*) denotes the action produced by material points outside system S_s.

The second law of mechanics,

$$m\frac{d\vec{v}}{dt}=\vec{F}\,, \tag{2}$$

defines the acceleration $\frac{d\vec{v}}{dt}$ of a point body with mass *m* acted upon by other bodies with a resultant force $\vec{F}$. Equation (2) is the differential equation of motion for a body with mass *m*. By summing the actions due to all material points (Figure 1) on the material point with mass m_i, in accordance with law (2) we obtain the differential equation of motion of the material point:

$$m_i\frac{d\vec{v}_i}{dt}=\sum_{k\neq i}^{N}\vec{F}_{ik}^{\,in}+\sum_{j=1}^{J}\vec{F}_{ij}^{\,ex}\,, \tag{3}$$

where the first term in the right-hand side of equation (3) is the action of all internal forces on material point m_i, whereas the second term is the similar action of all external forces.

We sum equations (3) over all *N* material points of system S_s:

$$\sum_{i=1}^{N}m_i\frac{d\vec{v}_i}{dt}=\sum_{i=1}^{N}\sum_{j=1}^{J}\vec{F}_{ij}^{\,ex}\,. \tag{4}$$

In summing equations (3), by virtue of the third law of mechanics (1) the sum of all internal forces is zero. That is why all internal forces $F_{ik}^{\,in}$ are absent from equation (4).

In mechanics, the moment of force *F* and the moment of momentum *mv* relative to some center *C* are considered as a product of *h* by force *F* or by momentum *mv*. Here, *h* is the distance from center *C* to force *F* or to momentum *mv*. In vectorial form, the moment of momentum for $m\vec{v}$ is defined as $\vec{r}\times m\vec{v}$, where the radius-vector $\vec{r}$ directed from the center *C* to the point with mass *m*. The angular momentum $\vec{r}\times m\vec{v}$ is also a vector. We denote this vector as $\vec{m}_C(m\vec{v})$; then, the angular momentum of the material point m_i in Figure 1 is

$$\vec{m}_C\left(m_i\vec{v}_i\right)=\vec{r}_i\times m_i\vec{v}_i\,. \tag{5}$$

Point "*C*" in Figure 1 is chosen coincidental with the center of mass of system S_s.

According to formula (5), the angular momentum $\vec{m}_C\left(m_i\vec{v}_i\right)$ is a vector perpendicular both to the velocity $\vec{v}_i$ and to the radius-vector $\vec{r}_i$ of the body m_i. Let us find now the relation between the angular momentum of a moving material point and the moment of forces acting on this body. To this end, we vectorially multiply the left and right sides of the differential equation of its motion (3) by the radius-vector $\vec{r}_i$ of the point m_i:

$$\vec{r}_i \times m_i \frac{d\vec{v}_i}{dt} = \sum_{k\neq i}^{N} \vec{r}_i \times \vec{F}_{ik}^{\,in} + \sum_{j=1}^{J} \vec{r}_i \times \vec{F}_{ij}^{\,ex} \ .$$

Then, in accord with designation (5), we obtain the dependence of the angular momentum of the point m_i on the moment of forces acting upon this point in the form:

$$\frac{d}{dt}\vec{m}_C(m_i\vec{v}_i) = \sum_{k\neq i}^{N} \vec{m}_C(\vec{F}_{ik}^{\,in}) + \sum_{j=1}^{J} \vec{m}_C(\vec{F}_{ij}^{\,ex}) \ . \tag{6}$$

We sum equation (6) over all N material points of system S_s:

$$\frac{d}{dt}\sum_{i=1}^{N} \vec{m}_C(m_i\vec{v}_i) = \sum_{i=1}^{N}\sum_{k\neq i}^{N} \vec{m}_C(\vec{F}_{ik}^{\,in}) + \sum_{i=1}^{N}\sum_{j=1}^{J} \vec{m}_C(\vec{F}_{ij}^{\,ex}) \ . \tag{7}$$

The left-hand side of equality (7) is the derivative of the total angular momentum of system S_s relative to the center C

$$\vec{M}_C = \sum_{i=1}^{N} \vec{m}_C(m_i\vec{v}_i) \ . \tag{8}$$

The first term in the right-hand side of equation (7) is defined by the internal forces $F_{ik}^{\,in}$. It can be shown that this term is zero, like in expression (4) on the summation of forces in (3) over all points m_i. Hence, with allowance for formula (8) the equation (7) can be written as

$$\frac{d\vec{M}_C}{dt} = \sum_{i=1}^{N}\sum_{j=1}^{J} \vec{m}_C(\vec{F}_{ij}^{\,ex}) \ . \tag{9}$$

Equation (9) presents the theorem about the change of the angular momentum for a system of interacting bodies.

Providing that system S_s is acted upon by no external bodies, or the action due to such bodies is neglected, that is $\vec{F}_{ij}^{\,ex} = 0$, then the right-hand side of equation (9) vanishes, and the angular momentum of system S_s remains unchanged, so that we have

$$\vec{M}_C = \text{const} \ . \tag{10}$$

Equation (10) is the law of conservation of the angular momentum.

In analyzing the dynamics and evolution of the Solar system, only the actions due to Solar-system bodies are to be taken into account. That is why the obtained solutions of the problems must comply with the law of conservation of angular momentum (10).

CHANGE OF ANGULAR MOMENTUM IN THE GALACTICA SYSTEM

Studying the motion of Apophis for different initial conditions and by different methods, we found [5] – [8] that the uncertainty of the asteroid's motion after approaching the Earth can be reduced by increasing methodological accuracy. Thus, we investigated the change of angular momentum of the Solar System in numerical calculations of its motion by two methods. The first method is traditional. It is based on the standard dynamic model (SDM) and is implemented in programs for calculating the DE series ephemeris, in particular the DE406 [9], and in the Horizons system [10]. The second method is implemented in the Galactica system [11] - [13]. It is based on the Newtonian interaction of point masses, and differential equations of motion are integrated using a new high-precision method. Information on the problems solved using the Galactica system can be obtained from: http://www.ikz.ru/~smulski/Papers/Galct11R.pdf. The Galactica system, with the functionalities necessary to solve problems, is freely available at http://www.ikz.ru/~smulski/GalactcW/. Its description is provided in the following files: GalDiscrp.pdf (Russian) and GalDiscrpE.pdf (English). The text of the program in Fortran was published in [13].

One important indicator for measuring the reliability of a solution of a differential motion equation is the dimensionless change of the system's angular momentum. In accordance with (10), in the absence of external influences on the system of interacting material points, the angular momentum of its motion in projection on the axis z, remains unchanged:

$$M_{Cz} = \sum_{i=1}^{N} m_i(v_{yi}\, x_i - v_{xi}\, y_i) = \text{const}, \qquad (11)$$

where m_i, x_i, y_i и v_{xi}, v_{yi} are the mass, coordinates, and velocities of the i-th body and N is the number of bodies in the system.

Therefore, the dimensionless change of the momentum:

$$\delta M_{Cz} = (M_{Cz} - M_{Cz0})/M_{Cz0}, \qquad (12)$$

where M_{Cz0} is the angular momentum at a certain point in time, must be zero; i.e., $\delta M_{Cz} = 0$. If it is not zero, we have evidence of errors in the numerical integration of the problem.

The measure of the accuracy of δM_{Cz} in the integration of equations in Galactica and the relationship of δM_{Cz} with the errors in the coordinates and velocities are detailed in [14], [15]. While solving differential equations, Galactica calculates various reliability criteria for the computed results, including the

dimensionless change of the momentum, δM_{Cz}. Repeated studies for the Solar System have found that the projections of angular momentum onto the axes x and y behave similarly to the projection of δM_{Cz}. Since this projection is close in value to a change in the modulus of the momentum, δM_C, below we consider δM_{Cz}.

The angular momentum was calculated in Galactica for the planets, Moon, Sun, and Apophis in barycentric equatorial coordinates for the epoch 2000.0 [6] - [8]. The calculations were made with a step of $dT = 10^{-5}$ year and an extended length of numbers (34 decimal places). The pattern of change of δM_{Cz} over 160 years is shown in Figure 2a. It is evident that this value changes linearly with time at an average rate of $d\delta M_{Cz}/dT = 1.5 \cdot 10^{-21}$ cyr^{-1}, where 1 cyr = 100 yrs. As already mentioned above, these results were obtained using numbers of extended length. When integrating the equation of motion using Galactica system with the double length of numbers (17 decimal places) over this time interval, the error of momentum δM_{Cz} varies in the range $\delta M_{Cz} = \pm 10^{-13}$, i.e., does not increase linearly with the increase in time needed to solve the problem. The algorithm of the Galactica system allows for error stabilization (if necessary) also in the case of the extended number length.

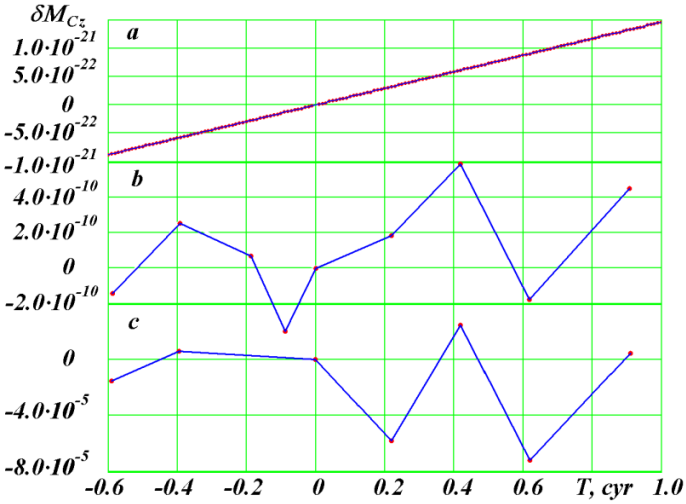

Figure 2. Dimensionless change of angular momentum of the Solar System: (*a*) differential equations of motion of the Sun, planets, Moon, and Aphophis were integrated by Galactica; motion of the planets, Sun, Moon, and the three asteroids (Ceres, Pallas, and Vesta) were calculated using, (*b*) DE406, and (*c*) Horizons. The values of δM_{Cz} were calculated from (12) at M_{Cz0} as of November 30, 2008. T is time in Julian centuries of 36525 days in a century, from the epoch of November 30, 2008.

CHANGE OF ANGULAR MOMENTUM IN THE SDM SYSTEM

We studied the change of angular momentum using the DE406 ephemeris and the Horizons system for the planets, the Sun, the Moon, and three asteroids Ceres, Pallas, and Vesta relative to the center of mass of the Solar System. We calculated the projections of the angular momentum M_{Cx}, M_{Cy} and M_{Cz} onto the axes of the barycentric equatorial frame and angular momentum modulus M_C. All the calculations were performed for several time points. The body masses for the DE406 ephemeris (the same as in the DE405 ephemeris) were taken from their description.

The Horizons system also assigns a mass to each body. Since these masses differ from those used in the DE406 ephemeris, we also calculated the angular momenta with the masses from the DE406 ephemeris. Moreover, Horizons has Pluto's coordinates until January 29, 2051. Therefore, we calculated the angular momenta without Pluto. However, it turned out that the pattern of change of the angular momenta in the two latter cases is virtually the same as in the first case. Thus, in our further work we used the angular momenta with the masses from the DE405 ephemeris.

Table 1 presents momenta M_{Cz} calculated using the DE406 ephemeris and Horizons for a period of 160 years. For the DE406 ephemeris, the values of the momentum are unchanged to the 10th significant digit; in the Horizons system, to their 4th significant digit. The pattern of change for the projections of momentum M_{Cx} and M_{Cy} and total momentum M_C is similar to the change in the *z*-projection of momentum M_{Cz}; therefore, in what follows, we consider, like in Galactica, only the projection of the momentum onto the *z* axis.

Table 1. Angular momentum M_{Cz} of the motion of the planets, the Sun, the Moon, and three asteroids, which was calculated using the DE406 ephemeris and the Horizons system for different dates and numbers of Julian days (JD) with the masses from DE405

Date	*JD*	$M_{Cz},\cdot 10^{+43}$ kg·m^2/s	
		DE406	Horizons
Dec. 30, 1949	2433280.5	2.884103707433978	2.884087593847136
June 28, 1969	2440400.5	2.884103708561933	2.884148971531926
Nov. 30, 2008	2454800.5	2.884103707836915	2.884131506700124
Nov. 30, 2030	2462835.5	2.884103708363054	2.883964569598089

Nov. 30, 2050	2470140.5	2.884103709521903	2.884202731605625
Nov. 30, 2070	2477445.5	2.88410370733108	2.883923748548167
Nov. 30, 2099	2488037.5	2.884103709125478	2.884144694607399

Figure 2 compares the changes in dimensionless angular momenta calculated using Galactica, DE406, and Horizons. The changes in momenta are given with respect to momentum as of November 30, 2008. The first point corresponds to December 30, 1949. As already noted, in Galactica the angular momentum grows linearly with time, and its change over 160 years was $\delta M_{Cz} = 2.4 \cdot 10^{-21}$. In the DE406 ephemeris, δM_{Cz} changes nonmonotonically, and the range of the variations is $8 \cdot 10^{-10}$, which is 11 orders of magnitude greater than the momentum in Galactica.

The angular momentum in Horizons also changes no monotonically, and the variations in δM_{Cz} can be as large as $9 \cdot 10^{-5}$. Hence it follows that, first, the changes in angular momentum in the DE406 ephemeris and in Horizons are many orders of magnitude greater than those in Galactica. Second, the changes in the angular momentum in Horizons are five orders of magnitude greater than those in the DE406 ephemeris.

It should be noted that originally the studies based on the DE406 ephemeris and the Horizons system were conducted for the planets, Moon, and Sun, i.e., without the three asteroids. The change in momentum δM_{Cz} for the DE406 ephemeris was greater by a factor of 2.5. The results in Table 1 and Figure 2 show a smaller change of δM_{Cz} because the DE406 based calculations took into account the three asteroids. Since the contribution of the asteroids to the change of the momentum δM_{Cz} is roughly $1.2 \cdot 10^{-9}$, it was expected that consideration of the asteroids would not affect the change of momentum in Horizons. This conclusion was confirmed by the calculations: consideration of the asteroids did not affect the error in angular momentum obtained using the Horizons system.

DYNAMICS OF ANGULAR MOMENTA OF SEPARATES BODIES

To understand the reasons for the change of angular momentum, we studied these changes using the DE406 ephemeris for individual bodies: the planets, Sun, and Moon. We considered the dimensionless change compared with the momentum as of November 30, 2008. We studied all the three projections of the momentum: δM_{Cx}, δM_{Cy} and δM_{Cz}. Since their behavior is identical, we considered, like in the above, only the projection onto the z axis. The change δM_{Cz}

for these bodies over 160 years is shown in Figure 3 with a solid line. It is clear that the angular momenta of the bodies, like those of the Solar System in Figure 2b, show oscillatory changes. The least dimensionless changes are observed for Pluto, Neptune, Saturn, and Jupiter. The Sun's momentum shows the greatest change, and among the planets the greatest change δM_{Cz} is observed for Mercury.

It should be kept in mind that, unlike in the two body problem, the interaction of more than two bodies results in a change of the angular momentum of each body. There is an ongoing exchange of momenta between the bodies. For example, it follows from the plots in Figure 3 that the values of δM_{Cz} for Jupiter (Jp) and the Sun (Su) change asynchronously, which is evidence of an exchange of angular momenta between these bodies. Thus, the problem is not that these momenta change, but how correctly the results of the integration reflect the actual changes in the bodies' angular momenta. A slight inconsistency between the calculated and actual values may lead, due to their summation, to a visible change of the angular momentum for the Solar System as a whole.

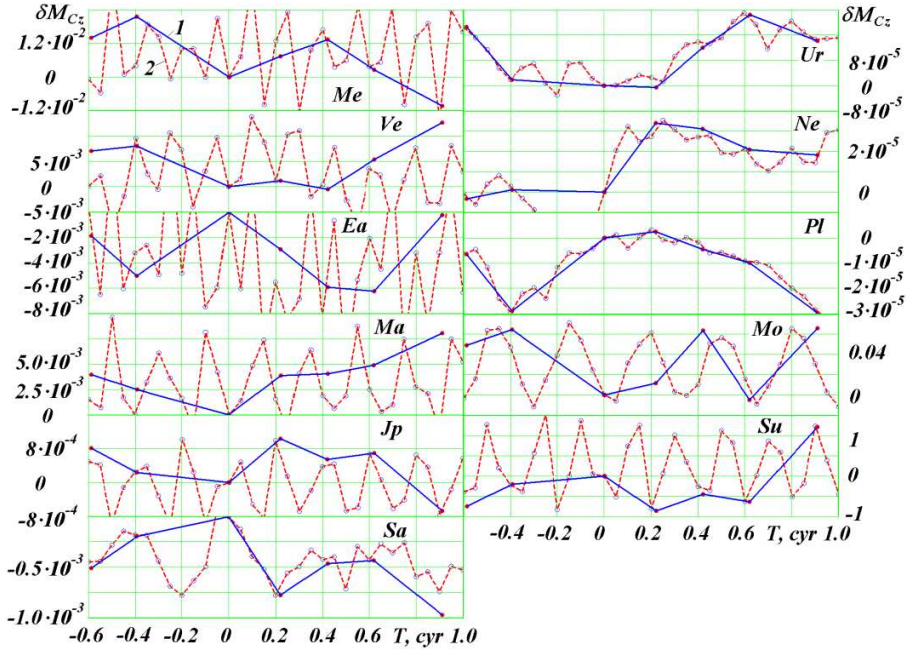

Figure 3. Dimensionless change of angular momenta for Solar System bodies from Mercury (*Me*) to the Moon (*Mo*) and Sun (*Su*). The value of δM_{Cz} was calculated from (2) at M_{Cz0} as of November 30, 2008: *1* using the DE406 ephemeris and *2* using Galactica.

The contribution of angular momenta of individual bodies to that of the Solar System depends on their absolute values. Table 2 shows the momenta $M_{Cz0,i}$ of the bodies, the range $\Delta\delta M_{Cz,i}$ of their dimensionless changes, and the range of the absolute changes $\Delta M_{Cz,i}$. These values were found from the formula:

$$\Delta\delta M_{Cz,i} = \delta M_{Czmax,i} - \delta M_{Czmin,i}; \quad \Delta M_{Cz,i} = M_{Cz0,i} \cdot \Delta\delta_{MCz,i}, \qquad (13)$$

where i is the number of the body and $\delta M_{Czmax,i}$ and $\delta M_{Czmin,i}$ are the maximum and minimum value of $\delta M_{Cz,i}$ in the plots in Figure 3.

It is evident that the largest absolute range $\Delta M_{Cz,i}$ of the variations in the angular momentum is observed for the Sun and Jupiter, and, as we see from Table 2, their $\Delta M_{Cz,i}$ are similar. As noted above, their momenta change in antiphase. Therefore, the errors in the determination of their angular momenta may contribute substantially to $\delta M_{Cz,i}$ of the Solar System as a whole.

Table 2. Ranges of change of the angular momentum for the planets, Moon, and Sun relative to Solar System center of mass using DE406 for a period of 160 years from December 30, 1949. The dimensionless changes were determined with respect to November 30, 2008. The projections of the bodies' angular momenta $M_{Cz0,i}$ and their changes $\Delta M_{Cz,i}$ are given in kg·m/s

Bodies' No.	1	2	3	4	5	6
body	Me	Ve	Ea	Ma	Jp	Sa
$\Delta\delta M_{Cz,i}$	0.0318	0.0132	0.00626	0.008	0.00172	0.000975
$M_{Cz,i}$	$7.795378332 \cdot 10^{38}$	$1.6744633 \cdot 10^{40}$	$2.4522183 \cdot 10^{40}$	$3.1839633 \cdot 10^{39}$	$1.7690015 \cdot 10^{43}$	$7.2208333 \cdot 10^{42}$
$\Delta M_{Cz,i}$	$2.4789303 \cdot 10^{37}$	$2.2076076 \cdot 10^{38}$	$1.5344546 \cdot 10^{38}$	$2.56960663 \cdot 10^{37}$	$3.0355753 \cdot 10^{40}$	$7.0420275 \cdot 10^{39}$
Bodies' No.	7	8	9	10	11	
body	Ur	Ne	Pl	Mo	Su	
$\Delta\delta M_{Cz,i}$	0.00231	0.000375	0.0000322	0.071	2.075	
$M_{Cz,i}$	$1.551594 \cdot 10^{42}$	$2.3175955 \cdot 10^{42}$	$3.6622486 \cdot 10^{38}$	$2.9202579 \cdot 10^{38}$	$1.5101363 \cdot 10^{40}$	
$\Delta M_{Cz,i}$	$3.5870122 \cdot 10^{38}$	$8.6886268 \cdot 10^{37}$	$1.1792440 \cdot 10^{34}$	$2.0741525 \cdot 10^{37}$	$3.1328189 \cdot 10^{40}$	

The same studies of angular momenta were conducted using the Galactica system. The dimensionless changes in momenta δM_{Cz} for the same bodies are shown in Figure 3 by a dashed line. Here the calculations were conducted with a smaller time interval, i.e., every five years. For planets with a large orbital period, beginning with Jupiter, the angular momentum is seen to change periodically. For the terrestrial planets, the variation periods δM_{Cz} are less than the five year

interval between the points in the plots. Therefore, one cannot see the variations of these periods.

When comparing the dimensionless momenta δM_{Cz} in the plots in Figure 3, which were calculated using the DE406 ephemeris and Galactica, it is evident that their dimensionless variation ranges are the same. In some cases, when the momenta are calculated for one and the same time point, the values of δM_{Cz} are also the same. For example, at $T \approx 0.4$ the dimensionless changes in the momentum have approximately the same values for the following bodies: Me, Ve, Ea, Jp, Sa, Ur, Ne, Pl, and Su. It is only for two bodies Mars (Ma) and the Moon (Mo) that they are visibly different. As is evident from Figure 2b, this difference for the DE406 ephemeris at $T \approx 0.4$ may lead to the largest error in angular momentum for the whole Solar System: $\delta M_{Cz} = 6 \cdot 10^{-10}$.

A good consistency in the changes of the momenta δM_{Cz} for the two programs over the entire range is observed for Uranus (Ur), Neptune (Ne), and the Sun (Su). At the same time, the momenta δM_{Cz} are observed to differ at around certain points in time: T = -0.6 and -0.4 for Mercury, T = -0.6 and 0.9 for Venus, T = 0.9 for Saturn, and T = 0.2 and 0.6 for the Earth and Mars. These differences in the angular momenta for individual bodies may lead to the previously observed variations in the angular momentum for the whole Solar System in the DE406 ephemeris. Thus, the comparisons of angular momenta for individual bodies (Figure 3) by different methods can serve as landmarks in searching for the reasons for errors in the less accurate program, i.e., the DE406 ephemeris.

DIFFERENCES IN THE POSITIONS OF BODIES

The calculated changes in angular momentum may indicate errors in the coordinates and velocities of bodies. We now try to estimate them. Let all bodies have the same dimensionless deviation δ for all coordinates and velocity components; then we can write the coordinate and velocity of the i-th body, i.e., for the projection onto the x axis, at any point in time:

$$x_i = x_{ti}\,(1 + \delta); \quad v_{xi} = v_{xti}\,(1 + \delta), \tag{14}$$

where x_i and v_{xi} are the calculated values and x_{ti} and v_{xti} the true values of the coordinate and velocity of the i-th body at this time point. If we substitute, according to (14), the coordinates and velocities into equation (11) for angular momentum and then into (12), we obtain

$$\delta M_{Cz} \approx 2\,\delta. \tag{15}$$

It should be noted that in this case the calculation of the dimensionless change in momentum δM_{Cz} is based on M_{Cz0} in (12), which is calculated from the true values of x_{ti} and v_{xti}, etc.

Thus, given that the dimensionless deviation of the coordinates and velocities is the same, it is half of the deviation of the momentum $\delta = 0.5\ \delta M_{Cz}$.

To analyze the structure of the deviations, we studied the differences between the DE406 ephemeris and the DE405, DE403, and DE200 ephemeris and the Horizons system for two dates: December 30, 1949 with the Julian day JD = 2433280.5 and December 30, 1999 with JD = 2451542.5. We determined the deviations of coordinates Δx_i, Δy_i and Δz_i and the velocities Δv_{xi}, Δv_{yi} and Δv_{zi} the deviations of the moduli of distances Δr_i and velocities Δv_i; and the angular displacement $\Delta\varphi_i$ in the plane xy and the dimensionless change in the distances between the positions of the body δr_i.

Table 3. Average dimensionless differences of the DE405, DE403, and DE200 ephemeris and the Horizons system from the DE406 ephemeris.

Source	Epoch Dec. 30, 1949		Epoch Nov. 30, 1999	
	δr_m	$\Delta\varphi_m$	δr_m	$\Delta\varphi_m$
DE405	$1.0\cdot10^{-11}$	$6.8\cdot10^{-12}$	$1.0\cdot10^{-11}$	$8.2\cdot10^{-12}$
DE403	$2.1\cdot10^{-7}$	$7.6\cdot10^{-8}$	$3.0\cdot10^{-7}$	$1.2\cdot10^{-7}$
DE200	$8.6\cdot10^{-7}$	$3.3\cdot10^{-7}$	$3.2\cdot10^{-6}$	$1.6\cdot10^{-7}$
Horizons	$1.9\cdot10^{-7}$	$1.5\cdot10^{-7}$	$1.1\cdot10^{-7}$	$5.2\cdot10^{-8}$

Table 3 gives two parameters of these studies, which were obtained by averaging over all bodies: δr_m is the average dimensionless deviation of the distance between the bodies in different calculation programs and $\Delta\varphi_m$ is the average moduli of the difference of the angular distances between the bodies in the heliocentric equatorial frame. As is evident from Table 3, these values are well correlated between each other, with $\Delta\varphi_m$ being approximately half as large as δr_m. A comparison of two different epochs 1949 and 1999 shows that the pattern of deviations is almost unchanged.

It is seen from Table 3 that the lower the number of an ephemeris, the worse is its accuracy. The data of Table 3 also confirm that the accuracy of the Horizons system is worse than that of DE406 or DE405 ephemeris. Moreover, it follows from the analysis of the differences in distances Δr and velocities Δv that although their values vary in a broad range for different bodies, their dimensionless values δr and δv vary within narrower limits. The average value of the limits is

accurately reflected by the values δr_m и and $\Delta\varphi_m$. Therefore, the use of the same value for the deviation . of the bodies' coordinates and velocities when deriving its dependence on the deviation δM_{Cz} of the angular momentum is justified.

When studying the changes in angular momentum over 160 years, we found that the range of its variations is $\Delta\delta M_{Cz} = 8\cdot10^{-10}$ for the ephemeris and $\Delta\delta M_{Cz} = 8\cdot10^{-10}$ for Horizons. Therefore, the dimensionless errors of the coordinates and velocities calculated using these systems should be expected to be of the order of $4\cdot10^{-10}$ and $4.5\cdot10^{-5}$, respectively. This accuracy estimate was obtained for the "true" parameters of the motion of the bodies, which give a constant angular momentum δM_{Cz}. Naturally, this estimate differs from the deviations δr_m in Table 3, which were obtained by comparing different versions of the ephemeris.

VARIATION OF ANGULAR MOMENTUM IN RECENT UPDATES OF DE EPHEMERIDES

The results shown in Figure 2 *b* and *c* were obtained in 2011. After the publication of our paper [16], the accuracy of the Horizons system was substantially improved and made comparable with that of the DE406 Ephemeris. The DE Ephemerides are being permanently improved and get updated almost every year. For example, the DE405 Ephemeris was released in 1998, and DE422, in 2009. That is why we have performed a study of the variation of angular momentum in the DE422 Ephemeris. In Figure 4, the variation of angular momentum according to the DE406 Ephemeris (curve *1*) is compared with the results of DE422 (curve *2*).

The graphs in Figure 4 show the variation of the projections of angular momentum, δM_{Cx}, δM_{Cy}, and δM_{Cz}, and also that of total angular momentum, δM_C, for the same Solar-system bodies as those shown in Figure 2. That is why for the projection δM_{Cz} of the DE406 Ephemeris (curve *1*) the graphs in Figures 2 and 4 are the same. Evidently, the magnitude of the oscillations of projection δM_{Cy} are the same as that for projection δM_{Cz}. The amplitude of the oscillations of projection δM_{Cx} is several times greater than that for δM_{Cz}. Yet, since the projection of angular momentum M_{Cx} is much smaller than M_{Cz}, the intense oscillations δM_{Cx} do not affect the oscillations δM_C of total angular momentum. That is why oscillations δM_{Cz} are almost perfectly coincident with oscillations δM_C. This result confirms the fact that the choice of quantity δM_{Cz} as an indicator of the accuracy of calculation programs for motions was made quite adequately.

When comparing the deviation of angular momentum of the later DE422 Ephemeris (curve *2*) with DE406, we see that in some cases, the deviations of δM_{Cy}, δM_{Cz} and δM_C are smaller in comparison with those in DE406. However, in general, over the entire interval of 160 years the magnitude of the deviation has even increased. This indicates that the DE Ephemerides have reached their utmost accuracy, and no future improvements will allow a reduction of errors at least by an order of magnitude.

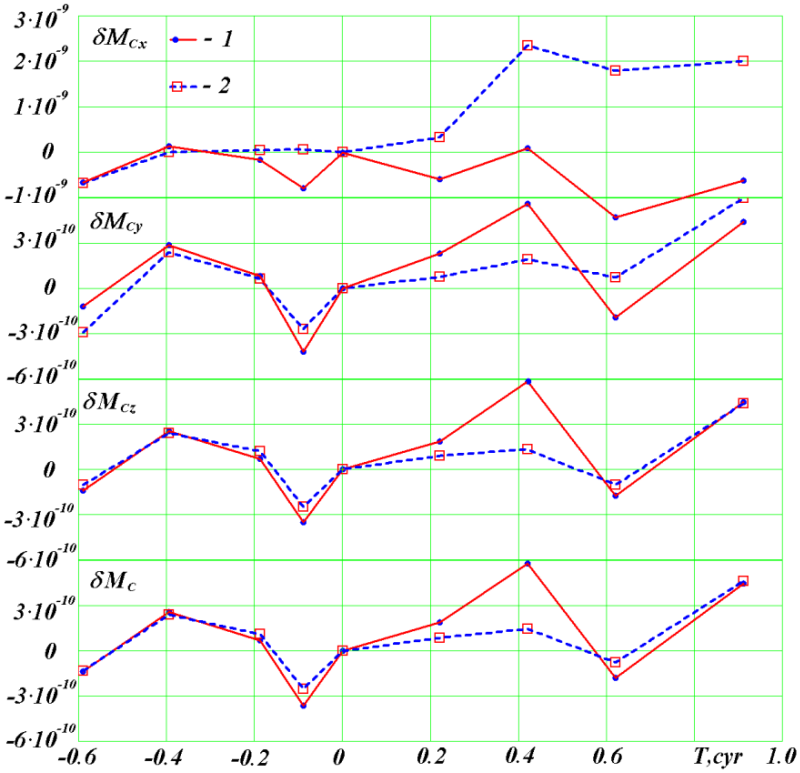

Figure 4. Dimensionless change of angular momentum of the Solar System: planets, Sun, Moon, and the three asteroids (Ceres, Pallas, and Vesta). *1* – DE406; *2* – DE422.

That is why we suggest that motions in the Solar system should be calculated using the Galactica program. The algorithm of this program has a considerable potential for improving the accuracy of calculation. Note that the actual error in calculating the position of bodies (or the difference of calculated position from actual position) is defined both by the starting data and by initial conditions.

Those data and conditions include the masses of bodies m_i, their coordinates $\vec{r}_{0i}$ and velocities $\vec{v}_{0i}$ at the initial time t_0. Subsequently, these values can be refined using the Galactica system throughout the entire observational base. Since there is no limit for such a refinement, there exists a good prospect for the long-term use and further development for the Galactica system.

VARIATION OF ANGULAR MOMENTUM OF PLANETS RELATIVE TO THE SUN

Above, we analyzed the variation of the angular momentum relative to the center of mass of the Solar system. When analyzing the motion of planets, their orbits are considered not relative to the center of mass, but relative to the Sun. In the problem of two bodies, the Sun and a planet, the angular momentum of the planet relative to the Sun experiences no changes [17]. The latter is also evidenced by the second Kepler law: the radius-vector of the planet describes equal areas over equal periods. In theoretical mechanics, this law is extended to all cases with a central force, i.e. the force that passes through the center of action.

The second Kepler law was established by Kepler, based on an analysis of the astronomical observations made by Tycho Brahe. This law reflects an approximate motion of the planets. It can be approximated with an ellipse, a flat and closed line. As a result of the joint action due to the Sun and other planets, the orbit of each planet presents an open spatial curve. Therefore, the angular momentum of a planet relative to the Sun undergoes variations.

We used Galactica to study with more detail, the change of angular momentum for the planets relative to the Sun. The angular momentum in projection on the axis *z* is defined by equation

$$M_{zi} = m_i(v_{Syi}x_{Si} - v_{Sxi}y_{Si}),$$

where x_{Si}, y_{Si} и v_{Sxi}, v_{Syi} are the coordinates, and velocities of the *i*-th planet relative to the Sun. The periodicity in the change of coordinates and velocities is due to periodicity in the movement of the planets. Since the period *P* of revolution of the planets changes a thousand fold from Mercury to Pluto, the studies were conducted at time intervals divisible by the period *P*. Figure 5 shows its change δM_z during one revolution of the planet. As is evident from the plots, the value δM_z for all planets in this interval undergoes oscillatory changes with periods less that *P* (planet's revolution). For the Earth (Ea), there are about 12 variations of δM_z, which are due to the lunar influence. The least variation range $\Delta\delta M_z \approx 3\cdot10^{-6}$

over the interval of one revolution is observed for Mercury, and the largest (if we ignore the Earth), for Jupiter: $\Delta\delta M_z \approx 2\cdot10^{-4}$. Due to lunar influence, the value $\Delta\delta M_z = 10^{-3}$ for the Earth is greater than for Jupiter.

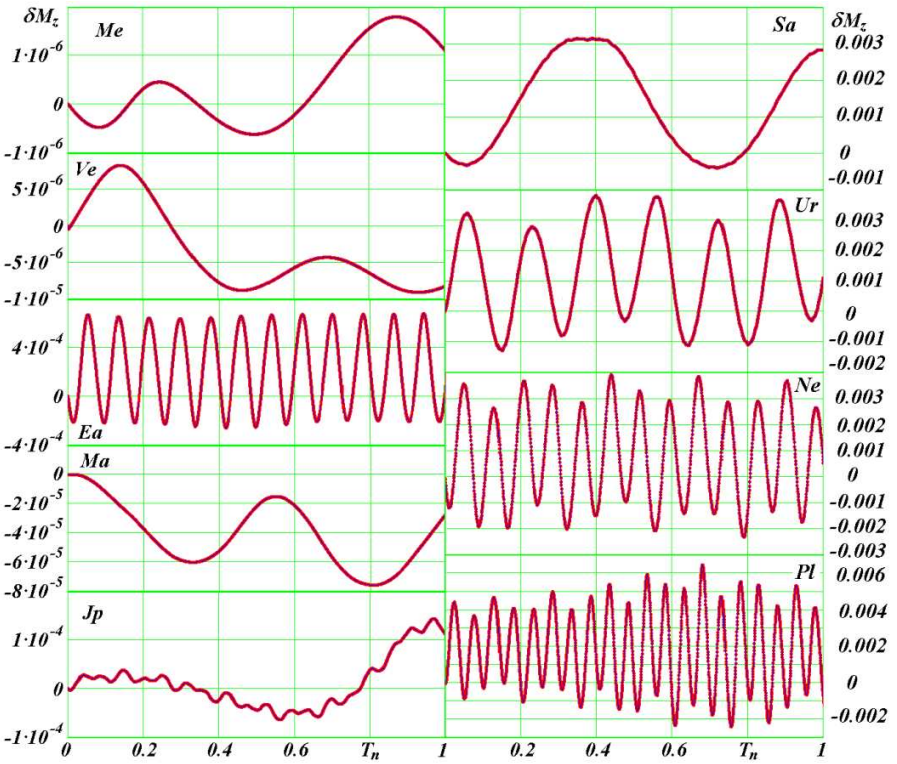

Figure 5. Dimensionless change of projection of angular momentum relative to the Sun for planets ranging from Mercury to Pluto over one orbital revolution. The values of δM_z were calculated at M_{z0} as of December 30, 1949. $T_n = T/P$ is the normalized time in orbital periods: P_{or} = 0.241, 0.615, 1.000, 1.88, 11.86, 29.42, 83.75, 163.72, and 248.02 are orbital periods in sidereal years for planets ranging from Mercury to Pluto.

From Figure 5, it is evident that more regular oscillations δM_z are exhibited by Earth and by the planets ranging from Saturn to Pluto. As already noted, the regular oscillations δM_z of the Earth are due to the influence of the Moon. The regular oscillations δM_z of the external planets are due to the action of the internal planets, of which Jupiter has the greatest influence.

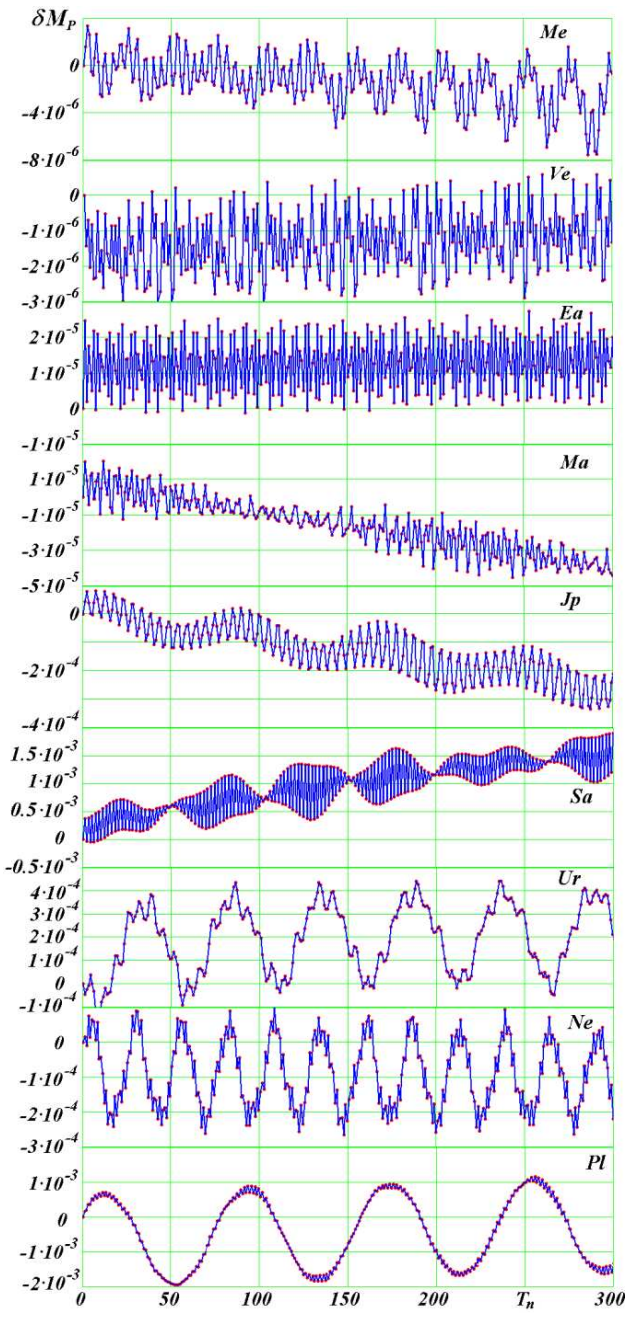

Figure 6. Dimensionless change of average modulus of angular momentum relative to the Sun for planets ranging from Mercury to Pluto over 300 orbital revolutions. The value of δM_P was calculated for average momentum modulus M_{P0} as of December 30, 1949.

The range of change of the angular momentum relative to the center of mass, $\Delta\delta M_{Cz}$ (this range is presented in Table 2) varies widely as well, from $\Delta\delta M_{Cz}$ = 0.0318 for Mercury to δM_{Cz} = 3.22 10^{-5} for Pluto. However, these values differ from the oscillations of angular momentum relative to the Sun. For Mercury, the oscillations relative to the Sun are 10000 times smaller, and for Pluto they are 300 times greater. This fact clearly indicates that the Sun, in its motion relative to the center of mass of the Solar

System, almost completely entrains Mercury into its motion. At the same time, the farthest planet Pluto is least susceptible to the Sun's orbital motion, its motion relative to the center of mass of the Solar system being more regular.

It should be noted that the dynamics of angular momentum δM_z during one revolution (Figure 5) can be different in a different epoch. Thus, we studied the changes in angular momentum over large time periods. We considered the average moduli of angular momenta δM_P during one revolution. These studies were carried out for each planet over an interval of 300 planetary revolutions. Figure 4 shows the changes in the average angular momenta for the same planets as in Figure 5. Since the interval between points in the plots in Figure 6 is one planetary orbital period P, the variation periods for angular momentum are equal to several periods P. For example, the least variation periods for the average angular momentum in Figure 6 for Mercury and Jupiter are 4 - 5 of their orbital periods P. As is seen from Figure 6, in addition to these short variations, there are also longer ones. And for Mars, Jupiter and Saturn one can see tendencies that mark the beginning of variations with a period of tens or hundreds of thousands of years. They are due to the long period variations of the planetary orbits [13] - [15].

For distant planets: Uranus, Neptune and Pluto, the oscillations of the angular momentum M_P (Figure 6) were established with periods of 5.125 kyr, 2.603 kyr and 8.033 kyr, respectively. With these periods, the parameters of the orbits of these planets also fluctuate. This includes the eccentricity, the angle of perihelion and the orbital period of the planet around the Sun. Fluctuations of the orbital period are fully identical to those of angular momentum. The range of variations of average angular momenta in Figure 6 does not exceed that of variations during one revolution, which are shown in Figure 5. The reason is that the averaging of variation amplitudes during one revolution reduces their range.

It should be noted that the high time resolution studies on angular momentum M_z using the Galactica system (Figure 5) show that the change δM_z for individual bodies is smooth, i.e., without any jumps or breaks. Therefore, the difference between δM_{Cz} calculated using DE406 (Figure 3) and those calculated using Galactica is due to inaccuracies in the DE406 ephemeris.

Thus, despite the various changes in angular momenta of the individual bodies of the Solar System, the angular momentum of the whole system relative to the center of mass C remains unchanged. The degree of change indicates the accuracy of the solution of equations describing Solar System dynamics. The Galactica gives the smallest change in angular momentum, and the Horizons system gives the greatest. The change of angular momentum of individual bodies

in the best program of calculation can serve as a benchmark to determine the causes of errors in those less accurate.

EVOLUTION OF ANGULAR MOMENTUM OF THE PLANETS OVER MILLIONS OF YEARS

While studying the evolution of the orbits of planets, we have established the fact that the angular momentum of the orbital motion of a planet relative to the Sun averaged over one rotation of the planet, $\vec{M}_p$, was perpendicular to the mean plane of the orbit [15], [18]. The study of the evolution of the orbits of the planets over millions of years has shown that the vectors of the angular momenta $\vec{M}_p$ of the planetary orbits precess relative to the angular momentum $\vec{M}_C$ of the entire Solar system. Figure 7 shows a frame $Ox_My_Mz_M$ whose axis z_M is directed along the vector $\vec{M}_C$. The differential equations of motion for Solar-system bodies are solved in the stationary equatorial frame *Oxyz* attached to the Earth's equatorial plane from the year 1950.0. The x_MOy_M plane is inclined to the *xOy* equatorial plane at the angle

$$i_M = \arccos(M_{Cz}/M_C) = 0.40183,$$

and the angle of the ascending node of the x_MOy_M plane is

$$\varphi_M = \pi/2 + \mathrm{arctg}(M_{Cy}/M_{Cx}) = 0.06809,$$

where M_{Cx}, M_{Cy} and M_{Cz} are the projections of $\vec{M}_C$ on the axes of the *Oxyz* equatorial system, and $M_C = \sqrt{M_{Cx}^2 + M_{Cy}^2 + M_{Cz}^2}$ is the absolute magnitude of $\vec{M}_C$.

The average for period the angular momentum of a planet $\vec{M}_p$ is perpendicular to the orbital plane of this planet. Therefore we introduce a unit vector $\vec{S}$ of the orbital axis, directed perpendicularly to the orbital plane. The projections of this vector are

$$S_x = M_{px}/M_p, \qquad S_y = M_{py}/M_p, \qquad S_z = M_{pz}/M_p, \tag{16}$$

where $M_p = \sqrt{M_{px}^2 + M_{py}^2 + M_{pz}^2}$, $S = \sqrt{S_x^2 + S_y^2 + S_z^2} = 1$, and M_{px}, M_{py}, and M_{pz} are the projections of the vector $\vec{M}_p$ on the axes of the equatorial baricentric coordinate system.

As it follows from Figure 7*a*, the projections of the orbital axis $\vec{S}$ on the axes of the inertial $Ox_My_Mz_M$ frame are

$$\begin{aligned} S_{xM} &= S_x \cdot \cos\varphi_M + S_y \cdot \sin\varphi_M; \\ S_{yM} &= S_x \cdot \sin\varphi_M \cdot \cos i_M + S_y \cdot \cos\varphi_M \cos i_M + S_z \cdot \sin i_M; \\ S_{zM} &= S_x \cdot \sin\varphi_M \cdot \sin i_M + S_y \cdot \cos\varphi_M \cdot \sin i_M + S_z \cdot \cos i_M. \end{aligned} \quad (17)$$

Figures 7*b* and 7*c* show the evolution of the Earth's orbital axis $\vec{S}$ in two planes, y_MOx_M and z_MOx_M. Figure 7*b* shows a segment of the trajectory of the end of the axis $\vec{S}$ over 400 ka. Starting from the time T = -400 kyr, the orbital axis rotates clockwise around the momentum vector $\vec{M}_C$, i.e. against the orbital motion of the Earth around the Sun. Precession of the axis $\vec{S}$ proceeds with a period T_S = 68.7 kyr, the average angular velocity per revolution being ω_S = -1885 "/cyr (1 cyr – 1 century). The trajectory made by the end of the vector in the x_MOy_M plane is an open two-oval curve. This shape is due to the nutational oscillations, i.e. due to the changes in the angle Θ_S (see Figure 7*a*) of the deviation of the orbital axis $\vec{S}$ from the momentum vector $\vec{M}_C$, which is defined as the quantity

$$\Theta_S = \arccos S_{zM}. \quad (18)$$

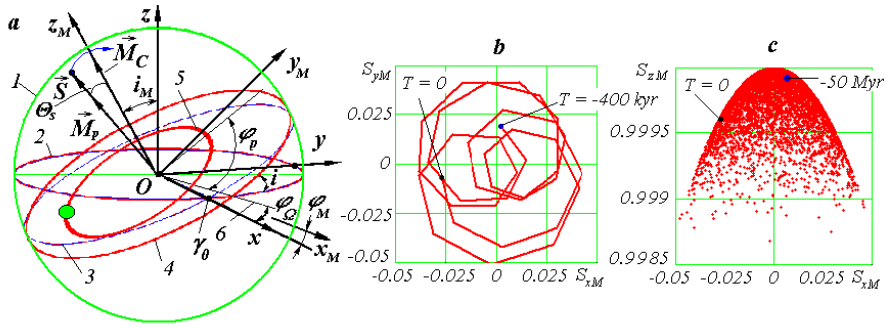

Figure 7. Precession of Earth's orbit axis $\vec{S}$ for 50 Myr. 1 Myr is 1 million years, and 1 kyr is 1 thousand years.

a. Coordinate system: *1* is the celestial sphere; *2, 3* are Earth's 1950.0 equatorial and orbital planes, respectively; *4* is Earth's orbital planes at epoch *T*; *5* is Earth's orbit at epoch *T*; *6* is the intersection of the moving orbital plane with the fixed equatorial plane**.**

b, c. Precession of the Earth's orbital axis in the plane y_Mx_M (solid line for -400 kyr) and in the plane z_Mx_M (red dots for -50 Myr). The large dots are positions of Earth's orbital axis at respective epochs. Data points are spaced at 10 kyr.

Precession of the vector $\vec{S}$ relative to the vector $\vec{M}_C$ is characterized by the precession angle

$$\psi_S = \text{arctg}S_{yM}/S_{xM} + 0.5\cdot\pi, \qquad (19)$$

which is reckoned (see Figure 7*a*) in the $x_M Oy_M$ plane from the x_M-axis to the ascending node *4* of the Earth's orbit on the $x_M Oy_M$ plane. The angle ψ_S is not shown in Figure 7*a*.

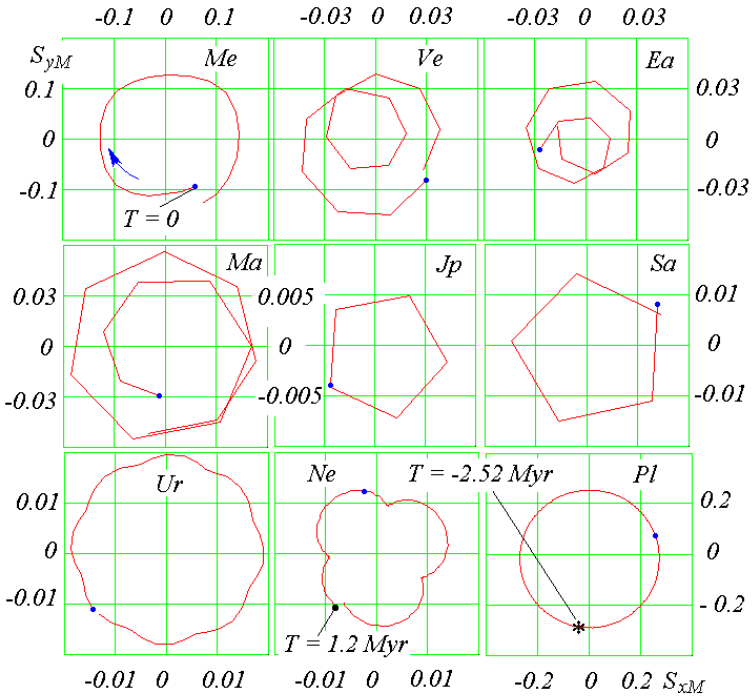

Figure 8. Precession of the planets' orbital axes for one revolution about the Solar System's angular momentum vector $\vec{M}_C$ from -2.56 Myr to +1.2 Myr (arrow shows the precession's direction); $T = 0$ corresponds to the 1950.0 frame and the path starting points, for planets from Mercury to Uranus; the paths for Neptune and Pluto start from past epochs.

From Figure 7*c*, it is seen that the change of projections S_{xM} and S_{zM} occurs symmetrically about the ordinate axis, i.e. relative to the angular momentum vector $\vec{M}_C$. In this case, the nutation angle Θ_S varies in the range $3.9\cdot10^{-4} < \Theta_S <$ 0.0514 radian, the average value being $\Theta_{Sm} = 0.0226$ radian. The maximum

deviation of the axis $\vec{S}$ from the angular momentum $\vec{M}_C$ makes an angle of Θ_{Smax} = 2.94º, and the range of nutational oscillations reaches 2·2.94º = 5.88º.

The main period of nutational oscillations is $T_{\Theta 1}$ = 97.35 kyr. Since that period is longer than the precessional period T_S = 68.7 kyr, i.e. it does not coincide with the latter period. Then the end of the axis $\vec{S}$ in Figure 7*b* describes a double oval trajectory. Note that there is a second period of nutational oscillations, equal to $T_{\Theta 2}$ = 1.164 million years.

So, the evolution of the Earth's orbital plane is due to the precessional motion of its orbital axis $\vec{S}$ around the angular momentum vector $\vec{M}_C$ with a period T_S = 68.7 kyr and due to the nutational oscillations of this axis occurring with a main period equal to $T_{\Theta 1}$ = 97.35 kyr.

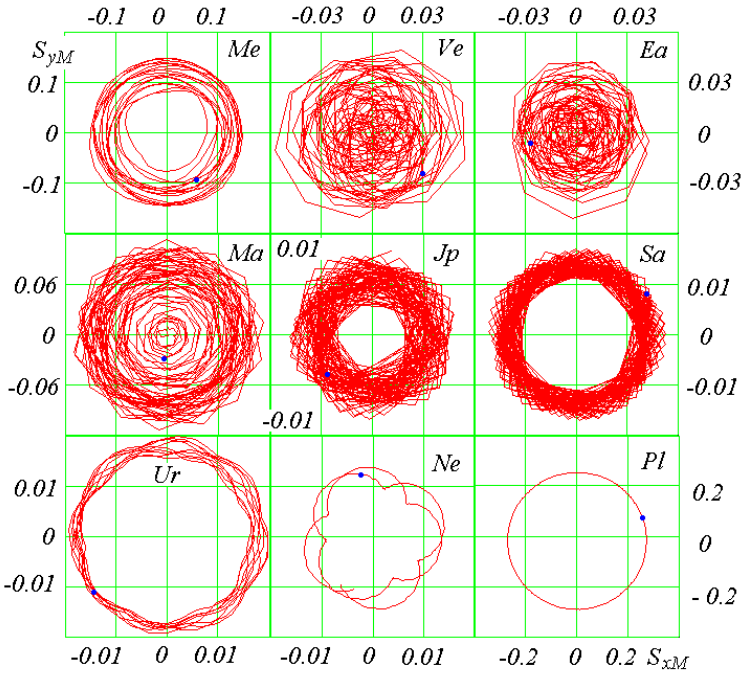

Figure 9. Precession of the orbital axes of the planets around the Solar System angular momentum vector $\vec{M}_C$ from -2.56 Myr to +1.2 Myr. Large dots mark the positions of the axes at T_0 = 1950.0.

The orbital axes of other planets in the Solar system execute similar precessional rotations and nutational oscillations (see Figure 8). The orbital axes

of all the planets revolve clockwise around the angular momentum vector $\vec{M}_C$, i.e. against the orbital motion. If the main period of nutational oscillations $T_{\Theta 1}$ exceeds the precessional period T_S and the nutational oscillations are significant, then the trajectory of the $S_{yM}(S_{xM})$ axis represents, as in the case of Venus, Earth and Mars, a two-oval trajectory. If the period of nutational oscillations $T_{\Theta 1}$ is several times shorter than the precessional period, then the trajectories of the axes, as in the case of Uranus and Neptune, are shaped as rosettes.

It should be noted here that the trajectories in the graphs of Figure 8 are depicted with straight lines connecting the points. Since the interval between the points is 10 kyr, then for a small precession period like, for instance, for Jupiter and Saturn with T_S = 50 kyr, the trajectories are represented by broken curves.

Figure 9 shows the precession of the axes of the orbits over 3.76 million years. We see that, during this period, the orbital axes of all the planets, with the exception of Pluto, make several turns: from 75 turns for the orbital axes of Jupiter and Saturn to 2 turns of the orbital axis of Neptune. Since the amplitudes of the nutational oscillations of the orbits of Venus, the Earth, and Mars are significant, the trajectories of their axes fill the central part of the $S_{yM}OS_{xM}$ plane. The smallest nutational oscillations are executed by the orbital axis of Pluto and, as a result, the trajectory of this planet turns out to be close to a circle.

Shown in Figure 10 is the precession of the axes of the orbits in three-dimensional form for the same period of time. In these graphs, the scale along the vertical axis is significantly increased. As it is evident from the graphs, the end of the unit vector $\vec{S}$ of the orbital axis for the first four planets describes surfaces convex at the center, and for the rest of the planets, annular surfaces.

Consider now in more detail the precession of the orbits. The precession angle ψ_S is to be calculated by formula (19). For many planets, the changes of ψ_S are not monotonous and, along with a decrease with time T (the axis $\vec{S}$ rotates in clockwise direction), there are intervals with increasing angle ψ_S. However, as it is shown by the points in Figure 11, over a long time interval of 50 million years no visible precession irregularities are observed. Shown here are appriximating dependences shown with thin lines:

$$\psi_{Sa} = \psi_{S0} + 2\pi \cdot T/T_S, \tag{20}$$

where ψ_{S0} is the value of the precession angle at the initial time $T = 0$; and

T_S are the precession periods of the orbital axes $\vec{S}$.

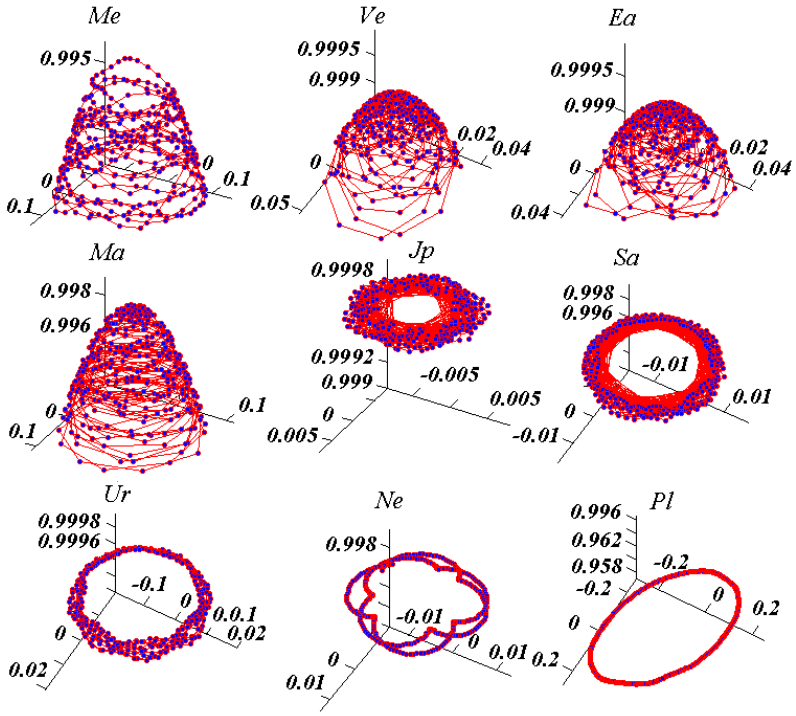

Figure 10. Precession of the orbital axes $\vec{S}$ of the planets around the Solar System angular momentum vector $\vec{M}_C$ from -2.56 Myr to +1.2 Myr, in 3D. The vertical axis is shifted parallel to the vector $\vec{M}$, and the axes origin is shifted from the origin of coordinates $OS_{yM}S_{xM}S_{zM}$.

The precession periods are represented in Figure 11 with numbers. Evidently, the values of ψ_S and ψ_{Sa} are coincident. From the presented data, it follows that the orbital axes of Jupiter and Saturn precess with the greatest velocity, and Pluto with the lowest velocity. For two groups of planets: Venus and Earth, Jupiter and Saturn, the rates of precession are almost coincident. We note once again that over small time intervals, the change in precession angles ψ_S differs from the linear law of (20).

Recall that the orbital axis $\vec{S}$ is the non-dimensional vector of angular momentum of the orbit $\vec{M}_p$ of Earth relative to the Sun. Therefore, it can be argued that the intricate behavior of Earth's orbital plane is explained by simpler

motions, the precession of Earth's orbital angular momentum $\vec{M}_p$ and its oscillations.

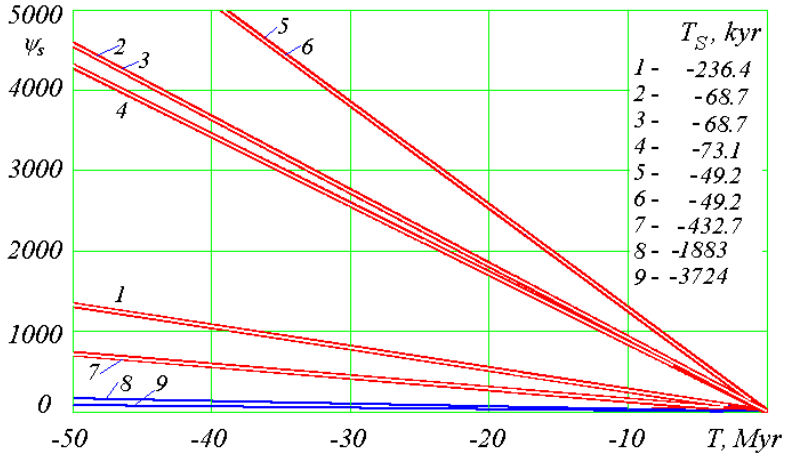

Figure 11. 50 Myr evolution of the precession angle ψ_S relative to the angular momentum $\vec{M}$ of the Solar System for nine planets from Mercury to Pluto (1 to 9), with the respective T_S periods in Kyr.

CHANGE OF ANGULAR MOMENTUM WITH REGARD TO THE ROTATIONAL MOTION OF BODIES

In the foregoing, we considered the total angular momentum of bodies in the dynamics of the Solar System, which is induced by their orbital motion. The consideration of the angular momentum induced by the rotational motion of bodies would expand the possibilities of this approach. For example, in the Earth-Moon system, one could trace an increase in the orbital angular momentum of the Moon due to the inhibition of the Earth's rotation. Therefore it is of interest to consider the total angular momentum, taking into account the angular momenta induced by the rotation of bodies. These angular momenta are also called spins of bodies. The above discussed programs for calculating only orbital motion do not consider the spins of bodies. Therefore, at this stage a study on changes of angular momentum in the dynamics of the Solar System can only be performed for orbital angular momenta.

It should be noted that the initial conditions in the Galactica system include, apart from orbital parameters, the radii of the bodies and the projections of their

spins. Therefore, if all of these parameters are specified for a problem of gravitational interaction of bodies, then solving this problem will give the dynamics of their orbital and rotational angular momenta. This analysis may cover collisions of bodies, their mergers into one body, collisions of the merged bodies, and other processes accompanying collisions.

These processes are complex, and it is rather difficult to choose and develop algorithms to describe them. In this case, control over the measurements of the total (including the spins) angular momentum is the only reliable method to control the accuracy of the results.

It should be noted that we consider the change of angular momentum in the dynamics of the Solar System, i.e., in theories describing the motion of the Solar System. A change of angular momentum in the Solar System depends not only on the orbital and rotational motion of bodies but also on other factors. The most important of them is orbital motion. In the future, with the increasing accuracy of the description of the first most important factors, the least important ones will also be taken into account.

Below we give an estimate for the angular momenta induced by the second most important factor, i.e., rotational motion of bodies. If J is the axial momentum of inertia and ω_{rt} is the angular velocity of rotation, then the spin of the body is

$$S_{rt} = J \cdot \omega_{rt} \approx 0.4\, m\, R^2 \cdot 2\pi / P_{rt} = 0.8\, \pi m \cdot R^2 / P_{rt}, \tag{21}$$

where m is the mass of the body; $J = 0.4\, m\, R^2$ is the axial momentum of inertia; R is its radius; and P_{rt} is its rotation period. If the average radius of the orbit is a and the angular velocity of the body's motion in orbit is ω_{or}, then its orbital angular momentum is

$$M_P = m \cdot \omega_{or} \cdot a^2 = 2\pi \cdot m \cdot a^2 / P, \tag{22}$$

where P is the orbital period of the body. Then the ratio of the spin to the orbital angular momentum is written as

$$S_{rt} / M_P = 0.4 \left(\frac{R}{a} \right)^2 \frac{P}{P_{rt}}. \tag{23}$$

Table 4 presents these ratios for the planets (from Me to Pl) and the Moon (Mo). The Moon's orbital angular momentum was calculated for its orbit around the Earth, and the planets' momenta, for their orbits around the Sun. It is evident that the orbital angular momentum is many orders of magnitude greater than the spin. Nevertheless, the accuracy of Galactica appears to be able to take the latter into account. Thus, in the future researchers will be able to pose problems and attempt to solve them using the Galactica system.

Table 4. Parameters of the planets from Mercury to Pluto (Me to Pl) and the Moon (Mo) and their average orbital momenta (M_P) and spins (S_{rt}). The "-" sign before the numbers indicates that the planet rotates clockwise.

Body	$m\cdot10^{-22}$, *kg*	*R*, thousand km	P_{rt}, days	*a*, million km	*P*, years	S_{rt}, kg·m^2/s	M_P, kg·m^2/s	S_{rt}/M_P
Me	33.019	2.4397	58.6462	57.909	0.2408	$9.748\cdot10^{29}$	$9.154\cdot10^{38}$	$1.06\cdot10^{-9}$
Ve	486.86	6.0519	-243.01	108.21	0.6152	$-2.134\cdot10^{31}$	$1.845\cdot10^{40}$	$-1.16\cdot10^{-9}$
Ea	597.37	6.3781	0.9973	149.60	1	$7.088\cdot10^{33}$	$2.662\cdot10^{40}$	$2.66\cdot10^{-7}$
Ma	64.185	3.397	1.026	227.94	1.8807	$2.1\cdot10^{32}$	$3.530\cdot10^{39}$	$5.95\cdot10^{-8}$
Jp	189900	71.492	0.4135	778.30	11.8565	$6.827\cdot10^{38}$	$1.932\cdot10^{43}$	$3.53\cdot10^{-5}$
Sa	56860	60.268	0.4375	1429.4	29.4235	$1.373\cdot10^{38}$	$7.861\cdot10^{42}$	$1.747\cdot10^{-5}$
Ur	8684.1	25.559	-0.65	2875.0	83.7474	$-2.539\cdot10^{36}$	$1.707\cdot10^{42}$	$-1.49\cdot10^{-6}$
Ne	10246	24.764	0.768	4504.4	163.7230	$2.38\cdot10^{36}$	$2.528\cdot10^{42}$	$9.41\cdot10^{-7}$
Pl	1.6509	1.151	-6.3867	5915.8	248.0208	$-9.961\cdot10^{28}$	$4.638\cdot10^{38}$	$-2.15\cdot10^{-10}$
Mo	7.3477	1.738	27.3217	0.38440	0.0748	$2.363\cdot10^{29}$	$2.89\cdot10^{34}$	$8.18\cdot10^{-6}$

EVOLUTION OF ANGULAR MOMENTUM OF ROTATIONAL MOTION OF EARTH OVER MILLIONS OF YEARS

As already noted, the orbital motion of Solar-system bodies proceeds in accordance with the law of conservation of angular momentum (10). The rotational motion behaves differently. For instance, due to the rotation around its axis, Earth is stretched in the equatorial region. Therefore, the Moon, the Sun and the planets produce the moments of forces that act on Earth; as a result, the angular momentum of Earth rotation undergoes changes in accordance with Theorem (9). From this theorem, the differential equations of rotational motion for Earth are derived [19].

The orbital and rotational motions of the Earth are schematically shown in Figure 12 [20]. Earth moves in an elliptical orbit around the Sun, which is in the focus of the ellipse. The smallest distance between the Earth and the Sun in perihelion is designated as R_p, and the greatest distance in aphelion, as R_a. The orbital motion of Earth proceeds counter-clockwise if you look at the orbit from the North Pole, *N*. The perpendicular to the plane of the orbit is designated as $\vec{S}$, and, as already mentioned, it is called the orbital axis. The axis $\vec{S}$ precesses around the vector of the angular momentum $\vec{M}_C$ of the entire Solar system in clockwise direction with a period of 68.7 thousand years.

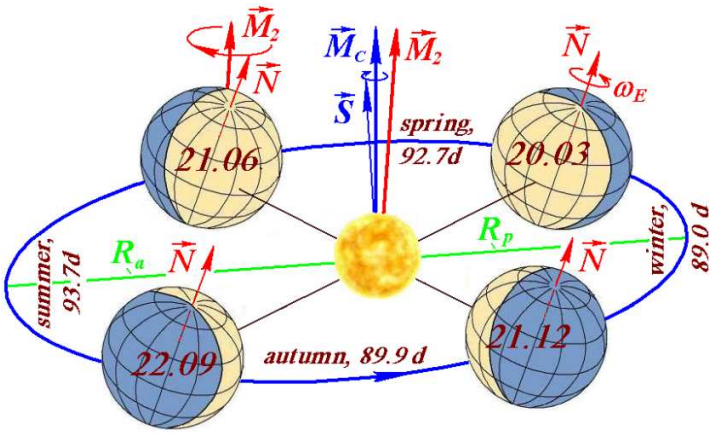

Figure 12. The Earth's positions in its orbit in 2025 at the days of the spring equinox (March 20), of the summer solstice (June 21), of the autumn equinox (September 22) and of the winter solstice (December 21), and the time of its movement in days in spring (92.7 d), in summer (93.7 d), in autumn (89.9 d) and in winter (89.0 d): $\vec{N}$ is the axis of the Earth's rotation, and $\vec{M}_2$ is the vector, relative to which the axis $\vec{N}$ precesses with a period of 25.74 thousand years; $\vec{S}$ is the axis of the Earth's orbit, and $\vec{M}_C$ is the vector relative to which the axis $\vec{S}$ precesses with a period of 68.7 thousand years [20].

The Earth rotates on its axis $\vec{N}$ in the same direction in which the Earth moves in its orbit, i.e., counter-clockwise. In the contemporary epoch, the axis $\vec{N}$ is inclined to the orbital axis $\vec{S}$ at the angle $\varepsilon = 23.443°$. As a result of solving the differential equations of Earth's rotational motion, it was found that the axis of Earth's rotation $\vec{N}$ precesses around a second direction in space, shown in Figure 12 with a vector $\vec{M}_2$ [20]. The precession period of the axis $\vec{N}$ is 25.74 thousand years. The vector $\vec{M}_2$ is inclined to the vector $\vec{M}_C$, around which the orbits of the planets precess, at an angle of 3.201402°. In term of direction, the angular momentum of the rotational motion of Earth almost coincides with the axis $\vec{N}$ of its rotation. Therefore, the motion of the vector $\vec{N}$ reflects the precession of the angular momentum due to Earth rotation.

The graph in Figure 13*a* shows, in the form of the dependence S_{yM} on S_{xM}, the precession of the orbital axis $\vec{S}$ around the vector of the angular momentum of

the Solar system $\vec{M}_C$ over a period of 5 million years. From starting point 1_S, the axis $\vec{S}$ moves into the past counter-clockwise, and to the future, its precession proceeds in a clockwise direction. Points 2_S and 3_S show the position of the axis $\vec{S}$ at other times. Over 5 million years, the precession mainly proceeds in such a way that the angle between the vectors $\vec{S}$ and $\vec{M}_C$ never exceeds 2.578°. Only in one precession cycle at point 2_S in epoch T = -2.326 kyr the angle between the vectors $\vec{S}$ and $\vec{M}_C$ reaches a value of 2.926°.

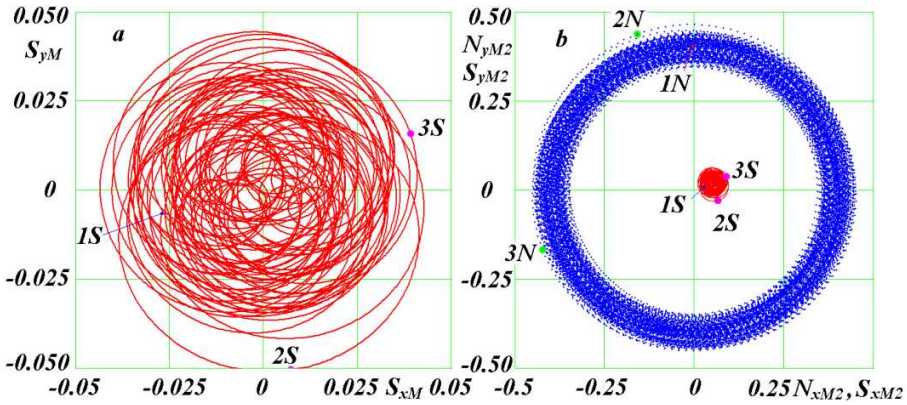

Figure 13. Projections of the precession trajectories of the Earth's orbital axis $\vec{S}$ (*a*) and its axis of rotation $\vec{N}$ (*b*) for 5 Myr on a plane perpendicular to the vectors $\vec{M}_C$ and $\vec{M}_2$, respectively. The positions of the axes at time points and angles between them: 1_S and 1_N for T = 0 kyr, ε = 23.443°; 2_S and 2_N for T = -0.2326 Myr, ε = 30.778°; 3_S and 3_N for T = -2.6582 Myr, ε = 32.680°.

The graph in Figure 13*b* illustrates, in the form of the dependence of N_{yM2} on N_{xM2}, the precession of the axis of Earth rotation $\vec{N}$ around the vector $\vec{M}_2$ over a period of 5 million years. Precession occurs within a ring with an average angle between the vectors $\vec{N}$ and $\vec{M}_2$ equal to θ_{M2} = 23.614°, the maximum angle being θ_{M2max} = 27.756°.

To compare the precessions of the axes of the Earth $\vec{N}$ and its orbit $\vec{S}$, projections S_{yM2} и S_{xM2} of the vector $\vec{S}$ in the $x_{M2}y_{M2}z_{M2}$ frame were determined. Figure 13*b* shows the motion of the axis of the Earth's orbit $\vec{S}$ with respect to the vector $\vec{M}_2$. The points 1_S, 2_S and 3_S show the position of the axis $\vec{S}$ in the

corresponding epochs. At the points 2_N and 2_S, the axes $\vec{N}$ and $\vec{S}$ are in one and the same epoch T = -0.2326 Myr. The large deviation of the orbital axis $\vec{S}$ has led to a large deviation in the Earth axis $\vec{N}$. However, the center of precession of the $\vec{S}$ axis is shifted in the perpendicular direction on line 2_N2_S of deviation of the axes $\vec{N}$ and $\vec{S}$ and, therefore, the angle between these axes in this epoch, ε = 30.778°, is not maximal. Over a period of 5 million years, the maximum angle ε = 32.68° occurs in the epoch T = -2.6582 Myr, when the line 3_N3_S coincides with the direction of deviation of the precession center of the $\vec{S}$ axis.

So, the angular momentum of the Earth's rotation and the angular momentum of its orbital motion both precess in a clockwise direction yet with different periods, 25.74 and 68.7 thousand years, respectively. Here, the axes of the precessions are different, and the angle between them is 3.201402°.

CONCLUSIONS

The translational motion of the material points of an isolated system, including the orbital motion of Solar-system bodies, proceeds in the analyzed statements without a change in the angular momentum of the entire system. Therefore, a change of this quantity in the calculation of motions indicates the error of the calculation method used. Here, the angular momenta of individual bodies undergo variation and the patterns of the variation for each body being individual. However, all the momenta precess around the angular momentum of the Solar system. The angular momenta due to the rotational motion of individual bodies also undergo variation. They also precess. However, the precession occurs relative to another direction in space.

The accuracy of the existing methods for calculating the motion of space objects is inadequate for today’s problems of space and celestial mechanics. For example, in order to improve the reliability of the calculated motion of Apophis after its encounter with the Earth in 2029, the accuracy of these methods should be increased by an order of magnitude [6], [7]. Researchers need more accurate methods, not only to calculate the motion of asteroids and spacecraft and to study the evolution of the Solar System over geological time intervals, but also for many other problems of celestial mechanics, e.g., to refine the masses of the planets. Our studies on the change of angular momentum make it possible to assess the accuracy of the methods used for calculating motions, find the causes of their errors and the ways to improve these methods.

ACKNOWLEDGMENTS

The materials of this work were obtained as a result of research at the Institute of Earth's Cryosphere, Tyum. SC of SB RAS for two decades, and in recent years, the research has been carried out under the project IX.135.2.4.

The Galactica calculations were performed using the supercomputers of the Siberian Supercomputer Center, Siberian Branch, Russian Academy of Sciences (SB RAS).

Careful reading and editing of the English text were made by Walter Babin, researcher and founder of the General Science Journal.

REFERENCES

1. Laskar, J. 1994. “Largescale chaos in the solar system.” *Astron. Astrophys.* vol. 287, no. 1, pp. L9–L12.

2. Rykhlova, L. V., Shustov, B. M., Pol, V. G. and Sukhanov, K. G. 2007. “Urgent problems in protecting the Earth against asteroids.” In *Proceedings of Intern. Conf. Near-Earth Astronomy 2007, September 3-7*, Terskol, Nal’chik, Russia, pp. 25-33.

3. Giorgini, J.D., Benner, L.A.M., Ostro, S.I., Nolan, H.C. and Busch, M.W. 2008. “Predicting the earth encounter of (99942) Apophis.” *Icarus*, vol. 193, pp. 1–19. http://dx.doi.org/10.1016/j.icarus.2007.09.012.

4. Anderson, J.D., Laing, P.A., Lau, E.L., Liu, A.S., Nieto, M.M. and Turyshev, S.G. 2002. “Study of anomalous acceleration of Pioneer 10 and 11.” *Phys. Rev. D*, vol. 65, 082004. http://journals.aps.org/prd/abstract/10.1103/PhysRevD.65.082004.

5. Smulsky, J.J. and Smulsky, Ya.J. 2010. “Evolution of Apophis orbit over 1000 years and new space targets.” In “*Protecting the Earth against Collisions with Asteroids and Comet Nuclei*,” Proc. of the Intern. Conf. “Asteroid–Comet Hazard – 2009”, Finkelstein, A., Huebner, W., and Shor, V., Eds., S.-Petersburg: Nauka, pp. 390– 395. http://www.ikz.ru/~smulski/Papers/EvlAp3Ec.pdf.

6. Smulsky, J.J. and Smulsky, Ya.J. 2011. “Evolution of Movement of Asteroids Apophis and 1950 DA for 1000 Years and their Possible Use.” *Institute of the Earth Cryosphere SB RAS.* - Tyumen. 36 p. - Figure: 10. Refer.: 27. - Russian. - Dep. In VINITI 25.01.11. No. 21-V2011. (In Russian) http://www.ikz.ru/~smulski/Papers/EvAp1950c.pdf.

7. Smulsky J.J. and Krotov O.I. 2011. “Computing of the Apophis's movement during 100 years on two approaches: Galactica and Horisons.” In *The Fundamental and Applied Problems of the Mechanics: Proceeding of the scientific Conference*, devoted 50-th anniversary of Yu. A. Gagarin's flight and 90-th anniversary of A.D. Kolmakov, the founder and the first director NII PMM TGU, April 12-14, 2011. - Tomsk: University Publishing House. Pp. 402-403. (In Russian). http://www.ikz.ru/~smulski/Papers/ClApGlH20.pdf.

8. Smulsky, J.J. and Smulsky Ya.J. 2012. “Asteroids Apophis and 1950 DA: 1000 years orbit evolution and possible use.” In *Horizons in Earth Science Research*, vol. 6, Veress, B., and Szigethy, J., Eds., USA: Nova Science Publishers, pp. 63–97. www.novapublishers.com/catalog/index.php.

9. Standish, E.M. 1998. “JPL Planetary and Lunar Ephemerides, DE405/LE405.” *Interoffice Memorandum: JPL IOM 312*. F98048, August 26,. ftp://ssd.jpl.nasa.gov/pub/eph/planets/ioms/de405.iom.pdf.

10. The HORIZONS System, http://ssd.jpl.nasa.gov/?horizons.

11. Smulsky, J.J. 2012. “Galactica software for solving gravitational interaction problems.” *Applied Physics Research*, vol. 4, no. 2, pp. 110–123. http://dx.doi.org/10.5539/apr.v4n2p110.

12. Smulsky J.J. 2012. The System of Free Access Galactica to Compute Interactions of N-Bodies. *I. J. Modern Education and Computer Science*, 11, 1-20. http://dx.doi.org/10.5815/ijmecs.2012.11.01.

13. Smulsky, J.J. 2018. *Future Space Problems and Their Solutions*. Nova Science Publishers, New York, 269 p. ISBN: 978-1-53613-739-2. https://novapublishers.com/shop/future-space-problems-and-their-solution.

14. Grebenikov, E.A. and Smulsky, J.J. 2007. “Evolution of the Mars Orbit on Time Span in Hundred Millions Years.” In *Reports on Applied Mathematics. Russian Academy of Sciences*, 63 p. (In Russian) http://www.ikz.ru/~smulski/Papers/EvMa100m4t2.pdf.

15. Melnikov, V.P. and Smulsky, J.J. 2009. *Astronomical Theory of Ice Ages: New Approximations. Solutions and Challenges.* Novosibirsk: Academic Publishing House “GEO”. http://www.ikz.ru/~smulski/Papers/AsThAnR.pdf.

16. Smul'skii, I.I. and Krotov, O.I. 2015. “Change of Angular Momentum in the Dynamics of the Solar System.” *Cosmic Research*, Vol. 53, No. 3, pp. 237-245. http://dx.doi.org/10.1134/S0010952515020094.

17. Smulsky, J.J. 1999. *The Theory of Interaction*. Novosibirsk: Publishing house of Novosibirsk University, Scientific Publishing Center of United Institute of Geology and Geophysics Siberian Branch of Russian Academy of Sciences. 294 p. http://www.ikz.ru/~smulski/TVfulA5_2.pdf – in Russian; http://www.ikz.ru/~smulski/TVEnA5_2.pdf – in English.

18. Smulsky, J.J. 2003. “The New Geometry of Orbits Evolution.” In *Proceeding of The Joint International Scientific Conference "New Geometry of Nature"*, August 25 - September 5, 2003, Kazan State University, Pp. 192-195. http://www.ikz.ru/~smulski/smul1/Russian1/IntSunSyst/NeGeEv2.doc (In Russian).

19. Smulsky, J.J. 2011. “The Influence of the Planets, Sun and Moon on the Evolution of the Earth's Axis.” *International Journal of Astronomy and Astrophysics*, 1, 117-134. http://dx.doi.org/10.4236/ijaa.2011.13017.

20. Smulsky, J.J. 2018. *New Astronomical Theory of Ice Ages*. “LAP LAMBERT Academic Publishing”, Riga, Latvia, 132 p. ISBN 978-613-9-86853-7. https://www.morebooks.de/store/ru/book/Новая Астрономическая теория ледниковых периодов/isbn/978-613-9-86853-7 (In Russian).